DOI: 10.1093/jnci/djr256
Advance Access publication on July 28, 2011.

ARTICLE

ABCC Multidrug Transporters in Childhood Neuroblastoma: Clinical and Biological Effects Independent of Cytotoxic Drug Efflux

Michelle J. Henderson, Michelle Haber, Antonio Porro, Marcia A. Munoz, Nunzio Iraci, Chengyuan Xue, Jayne Murray, Claudia L. Flemming, Janice Smith, Jamie I. Fletcher, Samuele Gherardi, Chin-Kiat Kwek, Amanda J. Russell, Emanuele Valli, Wendy B. London, Allen B. Buxton, Lesley J. Ashton, Alan C. Sartorelli, Susan L. Cohn, Manfred Schwab, Glenn M. Marshall, Giovanni Perini, Murray D. Norris

Manuscript received February 24, 2010; revised June 9, 2011; accepted June 16, 2011.

Correspondence to: Michelle Haber, AM PhD, Hon DSc, Children's Cancer Institute Australia for Medical Research, Lowy Cancer Research Centre, University of New South Wales, PO Box 81, Randwick, NSW 2031, Australia (e-mail: mhaber@ccia.unsw.edu.au) and Giovanni Perini, PhD,, Department of Biology, University of Bologna, via F. Selmi 3, 40126 Bologna, Italy (e-mail: giovanni.perini@unibo.it).

Background Although the prognostic value of the ATP-binding cassette, subfamily C (ABCC) transporters in childhood neuroblastoma is usually attributed to their role in cytotoxic drug efflux, certain observations have suggested that these multidrug transporters might contribute to the malignant phenotype independent of cytotoxic drug efflux.

Methods A v-myc myelocytomatosis viral related oncogene, neuroblastoma derived (*MYCN*)–driven transgenic mouse neuroblastoma model was crossed with an *Abcc1*-deficient mouse strain (658 $hMYCN^{+/-}$, 205 $hMYCN^{+/+}$ mice) or, alternatively, treated with the ABCC1 inhibitor, Reversan (n = 20). *ABCC* genes were suppressed using short interfering RNA or overexpressed by stable transfection in neuroblastoma cell lines BE(2)-C, SH-EP, and SH-SY5Y, which were then assessed for wound closure ability, clonogenic capacity, morphological differentiation, and cell growth. Real-time quantitative polymerase chain reaction was used to examine the clinical significance of *ABCC* family gene expression in a large prospectively accrued cohort of patients (n = 209) with primary neuroblastomas. Kaplan–Meier survival analysis and Cox regression were used to test for associations with event-free and overall survival. Except where noted, all statistical tests were two-sided.

Results Inhibition of ABCC1 statistically significantly inhibited neuroblastoma development in *hMYCN* transgenic mice (mean age for palpable tumor: treated mice, 47.2 days; control mice, 41.9 days; hazard ratio [HR] = 9.3, 95% confidence interval [CI] = 2.65 to 32; $P < .001$). Suppression of ABCC1 in vitro inhibited wound closure ($P < .001$) and clonogenicity ($P = .006$); suppression of ABCC4 enhanced morphological differentiation ($P < .001$) and inhibited cell growth ($P < .001$). Analysis of 209 neuroblastoma patient tumors revealed that, in contrast with *ABCC1* and *ABCC4,* low rather than high *ABCC3* expression was associated with reduced event-free survival (HR of recurrence or death = 2.4, 95% CI = 1.4 to 4.2; $P = .001$), with 23 of 53 patients with low *ABCC3* expression experiencing recurrence or death compared with 31 of 155 patients with high *ABCC3*. Moreover, overexpression of ABCC3 in vitro inhibited neuroblastoma cell migration ($P < .001$) and clonogenicity ($P = .03$). The combined expression of *ABCC1*, *ABCC3*, and *ABCC4* was associated with patients having an adverse event, such that of the 12 patients with the "poor prognosis" expression pattern, 10 experienced recurrence or death (HR of recurrence or death = 12.3, 95% CI = 6 to 27; $P < .001$).

Conclusion *ABCC* transporters can affect neuroblastoma biology independently of their role in chemotherapeutic drug efflux, enhancing their potential as targets for therapeutic intervention.

J Natl Cancer Inst 2011;103:1236–1251

Neuroblastoma, a cancer of embryonal neural crest cells, is the most common solid tumor of early childhood. The majority of children with neuroblastoma are diagnosed with advanced disease that is poorly responsive to conventional chemotherapy (1). Several biological and genetic factors have been identified for this disease, including age at diagnosis, tumor stage, unfavorable histology, and the status of the v-myc myelocytomatosis viral related oncogene, neuroblastoma derived (*MYCN*) oncogene (1). *MYCN* gene amplification can be demonstrated in approximately 20% of primary neuroblastomas, is accompanied by *MYCN* overexpression, and is a powerful adverse prognostic indicator for this disease (2,3).

The development of resistance to multiple cytotoxic drugs is a major cause of treatment failure in cancer patients, and members of the ATP-binding cassette (ABC) transporter superfamily, including ABC subfamilies B and C, member 1 (*ABCB1* and *ABCC1*), may contribute to this phenomenon by active efflux of chemotherapeutic agents from cancer cells (4). We have previously shown (5,6), both retrospectively and prospectively, that high-level expression of *ABCC1*, but not *ABCB1*, is a powerful independent prognostic indicator of poor outcome in neuroblastoma (5,6). Furthermore, *ABCC1* appears to be transcriptionally regulated by the *MYCN* oncogene in neuroblastoma cells (7,8). ABCC1 extrudes a number of chemotherapeutic drugs used in the routine treatment of neuroblastoma, leading us and others to conclude that ABCC1 may influence clinical outcome by mediating resistance to cytotoxic drugs used during treatment [reviewed in (4,9)]. Using two independent preclinical models of neuroblastoma, we recently demonstrated that genetic or pharmacological inhibition of ABCC1 sensitizes tumors to treatment with cytotoxic drugs that are known ABCC1 substrates (10).

However, there is also circumstantial evidence (11) that ABC transporters contribute to aspects of tumor biology independently of their capacity to expel cytotoxic drugs. In our own studies of *ABCC1* gene expression in primary untreated neuroblastoma, we have observed a small number of patients with favorable clinical stage neuroblastoma but with high-level expression of *ABCC1* and rapidly progressive disease (unpublished results). Because of their favorable clinical staging, these patients did not receive chemotherapy; therefore, the association between high *ABCC1* expression and clinical outcome cannot be explained in terms of ABCC1-mediated chemoresistance. Similarly, in a small retrospective study (12), we found that high levels of *ABCC4* expression, like *ABCC1*, were associated with poor clinical outcome in neuroblastoma, and although that same study demonstrated that high levels of ABCC4 could protect neuroblastoma cells from the chemotherapeutic drug irinotecan in vitro, the patients in the study received neither irinotecan nor any other drugs known to be ABCC4 substrates. Those results also suggested that the prognostic significance of *ABCC4* could not be explained in terms of ABCC4-mediated cytotoxic drug resistance. These findings raised the possibility that high levels of *ABCC1* and *ABCC4*, and potentially other ABC transporters, may contribute to poor outcome in neuroblastoma through functions additional to and independent of efflux of chemotherapeutic drugs.

To specifically address this hypothesis, we first examined the role of ABCC1 in tumor formation by inhibition or deletion of *Abcc1* in a well-characterized mouse model of neuroblastoma. We also tested the effects of depleting ABCC1 and ABCC4 using short interfering RNA (siRNA), or ectopic expression of ABCC1 and ABCC3, on cell motility, clonogenic capacity, differentiation, and cell growth in cultured neuroblastoma cells. Because other members of the ABCC branch of the ABC family can also extrude a variety of relevant physiological substrates, we examined the relationship between expression of all *ABCC* family members and clinical outcome in a large cohort of prospectively accrued neuroblastoma patients who had been previously recruited to assess *ABCC1*, as well as in a large independent cohort.

CONTEXTS AND CAVEATS

Prior knowledge

Resistance to cytotoxic drugs is thought to be a major cause of treatment failure in childhood neuroblastoma, and members of the ATP-binding cassette (ABC) transporter superfamily may contribute to this phenomenon by active efflux of chemotherapeutic agents from cancer cells. However, ABC drug transporters may also contribute to tumor progression through other mechanisms besides drug efflux.

Study design

The activity of the transporter ABC subfamily C, member 1 (ABCC1) was studied in mice null for ABCC1 or treated with an ABCC1 inhibitor. ABCC genes were also suppressed in neuroblastoma cell lines with short interfering RNA. The association of ABCC expression in tumor specimens with event-free and overall survival was analyzed in 209 primary neuroblastoma patients.

Contribution

Inhibition of ABCC1 suppressed neuroblastoma development in mice and inhibition of ABCC1 and ABCC4 suppressed clonogenicity and other functions relevant to tumor progression in neuroblastoma cell lines. Higher expression of ABCC1 and ABCC4 and lower ABCC3 expression were associated with higher rates of recurrence or death, as was the combined expression of all three transporters.

Implication

The ABC transporters ABCC1, 3 and 4 may contribute to poor outcomes in neuroblastoma through functions other than their role in resistance to cytotoxic drugs.

Limitations

The precise cellular mechanisms by which ABC transporters contribute to neuroblastoma progression are not yet known. In vivo experiments were only performed for the ABCC1 transporter but not for ABCC3 and ABCC4.

From the Editors

Materials and Methods

Transgenic and Knockout Mice and Treatment With Reversan

To examine the effect of ABCC1 on neuroblastoma development and progression, we used the *hMYCN* transgenic mouse, in which targeted expression of the *hMYCN* transgene to neuroectodermal tissue by use of a tyrosine hydroxylase promoter results in the development of neuroblastoma, which closely resembles the primary human disease (13). The transgenic mouse line was backcrossed for four generations to 129SV^{ter} mice (Animal Resources Centre, Perth, Australia) and maintained as an inbred line at Children's Cancer Institute Australia (14), with all subsequent male and female experimental mice being derived from this breeding colony. All mice that carry two copies of the transgene (ie, homozygous) develop tumors within a narrow 12-day window around 6 weeks of age. Recently, we identified a nontoxic, potent, and bioactive small-molecule inhibitor of ABCC1, designated Reversan, which enhanced the therapeutic efficacy of ABCC1-substrate drugs in tumor-bearing *hMYCN* transgenic mice (10). For ABCC1 inhibition studies, Reversan was obtained from ChemBridge Corp (San

Diego, CA). Weaned 3-week-old *hMYCN* transgenic mice were randomly assigned to treatment in a 5-day on and 2-day off schedule with either 10 mg/kg Reversan solubilized in dimethyl sulfoxide (DMSO) delivered by intraperitoneal injection (n = 20) or with equivalent amounts of the vehicle under the same schedule (control, n = 9), until a medium-sized palpable tumor (1 cm^2) was detected. This experimental design had more than 80% statistical power to detect a delay in tumor formation of at least 12%, at $\alpha = .05$.

The *hMYCN* transgenic mice were crossed with *Abcc1*$^{-/-}$ mice (C57 Bl/6 background), which have both alleles of *Abcc1* inactivated by homologous recombination (15). Offspring that were *hMYCN*$^{+/-}$*Abcc1*$^{+/-}$ were mated, and the resulting *hMYCN*$^{+/-}$*Abcc1*$^{+/-}$ offspring were then backcrossed four times to 129X1/SV mice (Jackson Laboratory, Bar Harbor, ME). A total of 658 *hMYCN*$^{+/-}$ mice (160 *Abcc1*$^{+/+}$, 329 *Abcc1*$^{+/-}$, and 169 *Abcc1*$^{-/-}$), in addition to 205 *hMYCN*$^{+/+}$ mice (50 *Abcc1*$^{+/+}$, 106 *Abcc1*$^{+/-}$, and 49 *Abcc1*$^{-/-}$), all on a 129 background, were followed to study variations in tumor incidence and latency associated with presence or absence of functional *Abcc1* alleles. Mice were palpated twice weekly and were killed by cervical dislocation or carbon dioxide–mediated asphyxiation when a medium-sized (1 cm^2) palpable tumor was detected. Tumor incidence was followed until the detection of a tumor or until 20 weeks of age. This experimental design afforded statistical power of at least 80% to detect a twofold decrease in tumor incidence at $\alpha = .05$ in a dominant genetic model.

All experimental procedures involving transgenic mice were approved by the University of New South Wales Animal Care and Ethics Committee according to the Animal Research Act, 1985 (New South Wales, Australia) and the Australian Code of Practice for Care and Use of Animals for Scientific Purposes (1997).

Gene Silencing, Transfection, and Cellular Assays

Human neuroblastoma cells BE(2)-C, SH-EP, and SH-SY5Y were obtained from the laboratory of Barbara Spengler (Fordham University, New York, NY) (16,17) and cultured in Dulbecco's modified Eagle medium (DMEM) containing 10% heat-inactivated fetal bovine serum and 2 mM glutamine. SH-EP cells were passaged 6–8 times before use. The identities of the BE(2)-C and SH-SY5Y lines were verified by short tandem repeat genetic profiling (CellBank Australia, Sydney, Australia).

Lipofectamine 2000 reagent (Invitrogen, Carlsbad, CA) was used to deliver SMARTpool siRNA or individual siRNA duplexes for *ABCC*1 (1–10 nM), *ABCC*4 (1–10 nM), or siCONTROL nontargeting pool siRNA (Dharmacon, Lafayette, CO) alone or in combination. For each cell line, siRNA transfection conditions were optimized using a green fluorescent protein–labeled siRNA duplex and flow-assisted cell sorting to determine conditions that would achieve transfection of at least 80% of cells. The siRNA sequences used as individual duplexes were, for ABCC1 suppression in SH-EP cells, ABCC1 SMARTpool duplex 1 (sense): GAUGACACCUCUCAACAAAdTdT; and for ABCC4 suppression in BE(2)-C cells, ABCC4 SMARTpool duplex 1 (designated ABCC4.1) (sense): GGACAGCCCUCGACCUUAAdTdT; or an independent sequence reported by Reid et al. (18), herein designated ABCC4 duplex 5 or ABCC4.5 (sense): GAUGGUGCAU GUGCAGGAUdTdT (18). For constitutive expression of ABCC1 in SH-SY5Y cells, transfection with pCMV14-3xFLAG-ABCC1, or the ATP-binding site mutants, pCMV14-3xFLAG-ABCC1-D1454N or ABCC1-DE1454LL, was followed by selection of stable clones with 500 μg/ml G418 (Geneticin; Invitrogen Australia Pty Ltd, Mulgrave, Australia), which were subsequently maintained with 150 μg/ml G418. The ABCC1-D1454N mutation was previously shown to abolish ATP-dependent ABCC1 transporter activity while not affecting correct localization of the transporter (19), and the ABCC1-DE1454LL mutant was predicted to have similar properties (Supplementary Figure 1, available online and http://www.uniprot.org/uniprot/O15439; accessed June, 2010). For stable clones expressing ABCC3, BE(2)-C cells were transduced with retroviral pCMV14-3xFLAG-ABCC3 or the ATP-binding site mutant, pCMV14-3xFLAG-ABCC3-V1322F. The V1322F mutation was predicted to abolish transporter activity while still being localized in the plasma membrane and is based on studies involving the closely related transporter, ABCC6, in which a single amino acid change in a region N-terminal to the Walker A motif in the second ABC domain abolishes catalytic activity (20) while retaining correct membrane localization in mammalian cell lines (Andras Varadi, personal communication). In this region, there is high sequence conservation with ABCC3. Localization of ABCC1 and ABCC3 variants to the plasma membrane was verified by immunocytochemical staining for the FLAG epitope (Supplementary Figures 1 and 2, available online). After G418 selection, pooled or cloned transfectants were examined for protein expression by western blot and immunocytochemistry. Control cells were stably transduced with an empty vector.

Generation of ATP-binding site mutants was carried out according to the QuikChange Lightning Site-Directed Mutagenesis Kit (Stratagene, La Jolla, CA) using forward primer 5′-ATC CTT GTG TTG AAT GAG GCC ACG GCA G-3′ for ABCC1-D1454N (single mutant), forward primer 5′-ATC CTT GTG TTG CTT CTG GCC ACG GCA G-3′ for ABCC1-DE1454/1455LL (double mutant) and forward primer 5′-AGG TGG GGA TCT TCG GCC GCA CTG G-3′ for ABCC3-V1322F.

Whole-cell extracts were prepared using lysis buffer (50 mM Tris pH 7.4, 150 mM NaCl, 0.2% NP-40, 50 mM NaF, 5 mM EDTA, 0.1 mM orthovanadate, plus protease inhibitor cocktail [Sigma]) as described previously (21). To analyze the expression of ABCC3 protein, membrane-enriched fractions were prepared using a published protocol (22). Western blots were performed according to standard procedures as previously described (5) using 20–50 μg of whole-cell or membrane extracts. The antibodies used were against ABCC1 (rat monoclonal MRPr1; Alexis Biochemicals, CA; 1:500), ABCC3 (mouse monoclonal M3II-21; Abcam number ab3376; Cambridge, MA; 1:750), ABCC4 (rat monoclonal M4I-10; Alexis Biochemicals; 1:1000), FLAG epitope (anti-FLAG mouse monoclonal M2; Sigma, St Louis, MO; 1:1000), ß-actin (rabbit polyclonal A2066; Sigma; 1:2000), and α-tubulin (mouse monoclonal DM1A; Sigma; 1:3000). Immunocytochemistry was performed using mouse monoclonal anti-FLAG M2 (Sigma) and Cy3-conjugated goat anti-mouse (Jackson Immuno Research, West Grove, PA). Nuclei were stained with Hoechst 33258 (Sigma). The intracellular localization of ABCC proteins was assessed using a conventional epifluorescence microscope (Eclipse 90i; Nikon Instruments, Melville, NY) equipped with a digital CCD camera. Image collages were made using Adobe Photoshop (Adobe System, Inc., San Jose, CA).

Unless otherwise stated, all means were derived from at least three experiments. For wound closure assays, cell-free areas were generated by use of either a pipette tip or removal of a wound assay chamber (IBIDI, Martinsried, Germany) 48–72 hours after siRNA transfection or 2–6 hours after Reversan (5 μM) addition, and once a confluent monolayer was present. Growth medium (DMEM) was replaced (with medium containing Reversan where applicable) and two or three wound areas per condition were photographed at 24 or 48 hours. Wound size was quantified by measuring the cell-free areas using Image-J software (National Institutes of Health, Bethesda, MD). To quantify neurite outgrowth, after 72-hour exposure to siRNA, cells with one or more neuritic extensions of at least twice the length of the cell body were scored as positive. At least 100 cells were counted per random field, with at least four fields taken per treatment in each of three separate experiments. Colony-forming assays were performed as previously described (23), with cells replated 24 hours following siRNA transfection and colonies of greater than 100 cells counted. Alternatively, 24 hours after plating, SH-EP cells were exposed to 5 μM Reversan for 72 hours and colonies counted 7 days after plating. DNA synthesis was monitored after 72-hour exposure to siRNA or 24-hour exposure to 5 μM Reversan. Cells in 12-well plates were cultured in the presence of 0.5 μCi of ^{3}H-thymidine and a 500-fold excess of unlabeled thymidine for 5 hours before harvesting for radioassay in triplicate by liquid scintillation counting. Bromodeoxyuridine (BrdU) incorporation was measured using a Delfia Cell proliferation kit (AD0200; Perkin Elmer, Waltham, MA). Cell clones were plated in 96-well plates at a cell density of 15 000 cells per well with 200 μL DMEM medium and cultured for 48 hours before addition of BrdU for 2–12 hours, followed by triplicate assay according to the manufacturer's protocol.

Patients and Tumor Specimens

The children in this study were enrolled in Pediatric Oncology Group (POG) Neuroblastoma Biology Study 9047 through POG-affiliated locations in North America, Switzerland, and Australia and were treated according to disease stage, age, and tumor biology, as specified in institutional as well as different POG protocols (5). To be eligible for POG Study 9047, patients were required to be 21 years of age or younger, newly diagnosed with pathological confirmation of neuroblastoma, to have informed consent, and to submit a blood or tumor specimen. Patients were consecutively accrued and, at the time of analysis, those specimens for whom clinical follow-up data were unavailable were excluded from the study. The final cohort comprised 209 patients (205 enrolled between 1996 and 1998 and four patients enrolled between 1994 and 1995). This study population was found to be representative of patients with neuroblastoma in general with respect to well-established prognostic indicators, including MYCN amplification status, age at diagnosis, and tumor stage (Supplementary Figure 3, available online). The median period of follow-up for surviving patients was 55 months (range 0–196 months), whereas the median time from diagnosis to death among the patients with treatment failure was 18 months (range 0–60 months). All deaths except for five (two attributable to infection and three to hemorrhage) were disease related. The protocol was approved by individual institutional review boards, and informed consent was obtained for every patient registered in the study.

Gene Expression Analyses

RNA was extracted using TRIZOL reagent (Life Technologies, Mulgrave, Australia) and reverse transcribed with Moloney murine leukemia virus reverse transcriptase (Life Technologies) according to the manufacturer's protocols, as previously described (5). Gene expression was determined by real-time quantitative polymerase chain reaction for 40 cycles using the ABI PRISM 7700 and ABI 7900HT sequence detection systems (Applied Biosystems, Foster City, CA). For each gene, transcript quantification was based on the comparative threshold cycle method, or ΔΔCt method, which compares the expression of a target gene normalized to the expression of a reference gene (in our case *ß$_2$-microglobulin*), to provide relative quantification (24). As a positive control for each assay, cDNA derived from either the IMR-32 or SH-EP neuroblastoma cell lines was included in the experiment. Primer and probe sequences for *ß$_2$-microglobulin* (internal control), *ABCC1*, and *ABCC4* (5,12) are listed, along with the remaining genes in Supplementary Table 1 (available online). Genes with a mean Ct value of 35 or greater in a set of 16 tumors (representative in terms of clinical parameters such as MYCN amplification status, stage, and clinical outcome) were not studied further.

Statistical Procedures

Differences in polymerase chain reaction values for a given target gene or phenotypic traits between groups were assessed by two-sided Student *t* tests. In the case of BrdU or ^{3}H-thymidine incorporation assays, one-sample Student *t* tests were used to compare between control and treated samples, where the control was assigned a value of 100%. For experiments involving more than two groups, one-way analysis of variance (ANOVA) was performed and, in cases where significant differences were detected, followed by pairwise *t* tests as indicated. Associations between clinical characteristics of patients and molecular characteristics of tumors were examined using Fisher's exact test. Event-free survival time was calculated as the time from diagnosis until the first occurrence of disease relapse, progression, death from any cause, or until last contact if no event occurred. Overall survival was the time from diagnosis until death or until last contact if the patient did not die. Survival analyses using SAS Version 9 (SAS Institute, Inc, Cary, NC) were performed according to the method of Kaplan and Meier (25) with SEs according to Peto and Peto (26) and comparisons of survival curves made using two-sided log-rank tests. Multivariable Cox regression analyses were performed to determine whether *ABCC1*, *ABCC3*, and *ABCC4* gene expression were independently statistically predictive of event-free or overall survival. For the publicly available microarray dataset, clinical, pathological, and gene expression data for 251 primary neuroblastoma tumors (27) were downloaded via http://pob.abcc.ncifcrf.gov/cgi-bin/JK; accessed January, 2009. Kaplan–Meier survival analyses were performed using StatView 4.1 (Abacus Concepts, Inc, Berkeley, CA). Probabilities of survival and hazard ratios (HRs) are given with 95% confidence intervals (CIs). Proportionality was confirmed by visual inspection of the plots of log(−log(S(time))) vs log(time), which were observed to remain parallel. *P* values less than .05 were

considered statistically significant. The clinical characteristics and outcomes of the patients were masked from the laboratory staff performing the gene expression analyses. For each of the genes analyzed, a continuous range of polymerase chain reaction values was obtained for the cohort of tumors. For a given gene, to categorize expression as either high or low, the cohort was repeatedly divided into two groups, with cut points at each quartile and at the lower and upper deciles of expression. For each cut point, a Cox model produced a *P* value and hazard ratio. Of the cut points with $P < .05$, the one with the highest hazard ratio was selected as the optimal expression cut point. This methodology has been described in detail in London et al. (28).

Results

Pharmacological or Genetic Attenuation of ABCC1 and Neuroblastoma Development In Vivo

To examine the effect of ABCC1 on neuroblastoma development and progression, we administered Reversan to *hMYCN* transgenic mice (n = 20; control group, n = 9) homozygous for the *hMYCN* transgene immediately after weaning but before macroscopic tumor development and in the absence of chemotherapeutic agents. We observed a statistically significant delay in tumor progression (mean age at occurrence of palpable abdominal tumor: treated mice, 47.2 days; vehicle-treated control mice, 41.9 days; HR = 9.3, 95% CI = 2.65 to 32; $P < .001$; Figure 1, A). To explore the role of ABCC1 in tumorigenesis, mice lacking the *Abcc1* gene ($Abcc1^{-/-}$) were crossed with *hMYCN* transgenic mice and the progeny monitored for tumor formation. Loss of one allele of *Abcc1* ($Abcc1^{+/-}$), and hence reduced expression of ABCC1 (Supplementary Figure 4, available online), resulted in an increase in tumor latency in mice homozygous for the *hMYCN* transgene by comparison with wild-type (wt) $Abcc1^{+/+}$ mice (mean age for occurrence of palpable abdominal tumor: $Abcc1^{+/+}$ mice [n = 50], 8.2 weeks; $Abcc1^{+/-}$ mice [n = 106], 9.2 weeks; HR = 1.63, 95% CI = 1.24 to 2.7; $P = .003$). Surprisingly, the statistical significance of this effect was lost upon complete deletion of *Abcc1* (mean age for occurrence of palpable abdominal tumor: $Abcc1^{+/+}$ mice [n = 50], 8.2 weeks; $Abcc1^{-/-}$ mice [n = 49], 8.6 weeks; HR = 1.1, 95% CI = 0.7 to 1.6; $P = .7$). Loss of one allele of *Abcc1* also decreased tumor incidence in mice hemizygous for *hMYCN* by comparison with mice possessing both alleles of *Abcc1* (tumor incidence: $Abcc1^{+/-}$ mice [n = 329], 12%; $Abcc1^{+/+}$ mice [n = 160], 21%; OR = 1.88, 95% CI = 1.13 to 3.11; $P = .02$, Fisher exact test; Figure 1, B). In mice completely lacking *Abcc1*, there was no further impact on incidence by comparison with mice lacking one allele of *Abcc1* (tumor incidence: $Abcc1^{+/-}$ mice [n = 329], 12%; $Abcc1^{-/-}$ mice [n = 169], 15%; OR = 1.3, 95% CI = 0.77 to 2.24; $P = .33$, Fisher exact test; Figure 1, B).

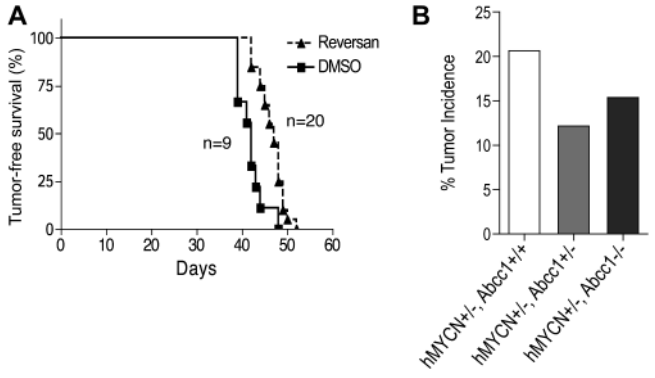

Figure 1. Role of ABCC1 in neuroblastoma formation in vivo. **A**) Administration of ABCC1 inhibitor, Reversan (**triangles**), and tumor formation in homozygous *hMYCN* transgenic mice (n = 20) and vehicle-treated controls (n = 9, DMSO; **squares**). **B**) Loss of one *Abcc1* allele ($Abcc1^{+/-}$) and tumor incidence in hemizygous *hMYCN* transgenic mice ($hMYCN^{+/-}$) compared with mice possessing both alleles of *Abcc1* ($Abcc1^{+/-}$ mice, n = 329, $Abcc1^{+/+}$ mice, n = 160, $P = .02$, two-sided Fishers exact test). Effect of loss of the second allele ($Abcc1^{-/-}$) compared with mice lacking one allele of *Abcc1* ($Abcc1^{+/-}$ mice, n = 329, $Abcc1^{-/-}$ mice, n = 169, $P = .33$; two-sided Fisher exact test). *Abcc1 = ATP-binding cassette, subfamily C, member 1*; DMSO = dimethyl sulfoxide; *hMYCN = human v-myc myelocytomatosis viral related oncogene, neuroblastoma derived.*

ABCC1 and ABCC4 Expression and Neuroblastoma Cell Biology

In light of these observations and our previous finding that high *ABCC4* expression is associated with poor outcome in neuroblastoma patients not treated with any drugs known to be substrates of ABCC4 (12), we sought to investigate the roles of ABCC1 and ABCC4 in neuroblastoma cell biology. Efficient depletion of ABCC1 and ABCC4 was achieved using siRNA in the *MYCN*-amplified human neuroblastoma cell line, BE(2)-C (Figure 2, A).

ABCC1 depletion led to impaired cell motility, as measured by the ability to move into an artificial wound (mean % of wound open ± 95% CI: ABCC1, 38.6 ± 6.9 vs control, 7.0 ± 3.5, $P < .001$, two-sided Student *t* test, four independent experiments; Figure 2, B and C). The decreased wound-filling ability was attributable to impaired cell motility rather than decreased proliferation, because cells depleted of ABCC1 showed only a modest, although statistically significant decrease in thymidine incorporation (mean % of control ± 95% CI: ABCC1, 91.7 ± 1.4; $P = .01$, one-sample Student *t* test, three independent experiments; Figure 2, D). The BE(2)-C cells depleted of ABCC1 also displayed a substantial impairment in colony-forming ability (mean number of colonies ± 95% CI: ABCC1, 19.8 ± 2.7 vs control, 26.0 ± 3.3, $P = .006$, two-sided Student *t* test, three independent experiments; Figure 2, E), whereas morphological differentiation, as assessed by neurite extension, was only slightly increased (mean % neurite-positive cells ± 95% CI: ABCC1, 4.3 ± 0.78 vs control, 2.0 ± 0.4, $P = .02$, two-sided Student *t* test, three independent experiments; Figure 2, F).

By contrast with ABCC1, depletion of ABCC4 from BE(2)-C cells resulted in markedly increased morphological differentiation (mean % neurite-positive cells ± 95% CI: ABCC4, 14.2 ± 2.4 vs control, 2.0 ± 0.4, $P < .001$, two-sided Student *t* test, three independent experiments; Figure 2, F). ABCC4 depletion was also associated with substantially decreased thymidine incorporation (mean % of control ± 95% CI: ABCC4, 62.3 ± 5.5, $P = .005$, one-sample *t* test, three independent experiments; Figure 2, D) and colony-forming ability (mean number of colonies ± 95% CI: ABCC4, 17.8 ± 2.6 vs control, 26.0 ± 3.3, $P < .001$, two-sided Student *t* test, three independent experiments; Figure 2, E). There was also some impairment of cell motility in ABCC4-depleted cells (mean % of wound open ± 95% CI: ABCC4, 26.5 ± 8.0 vs control,

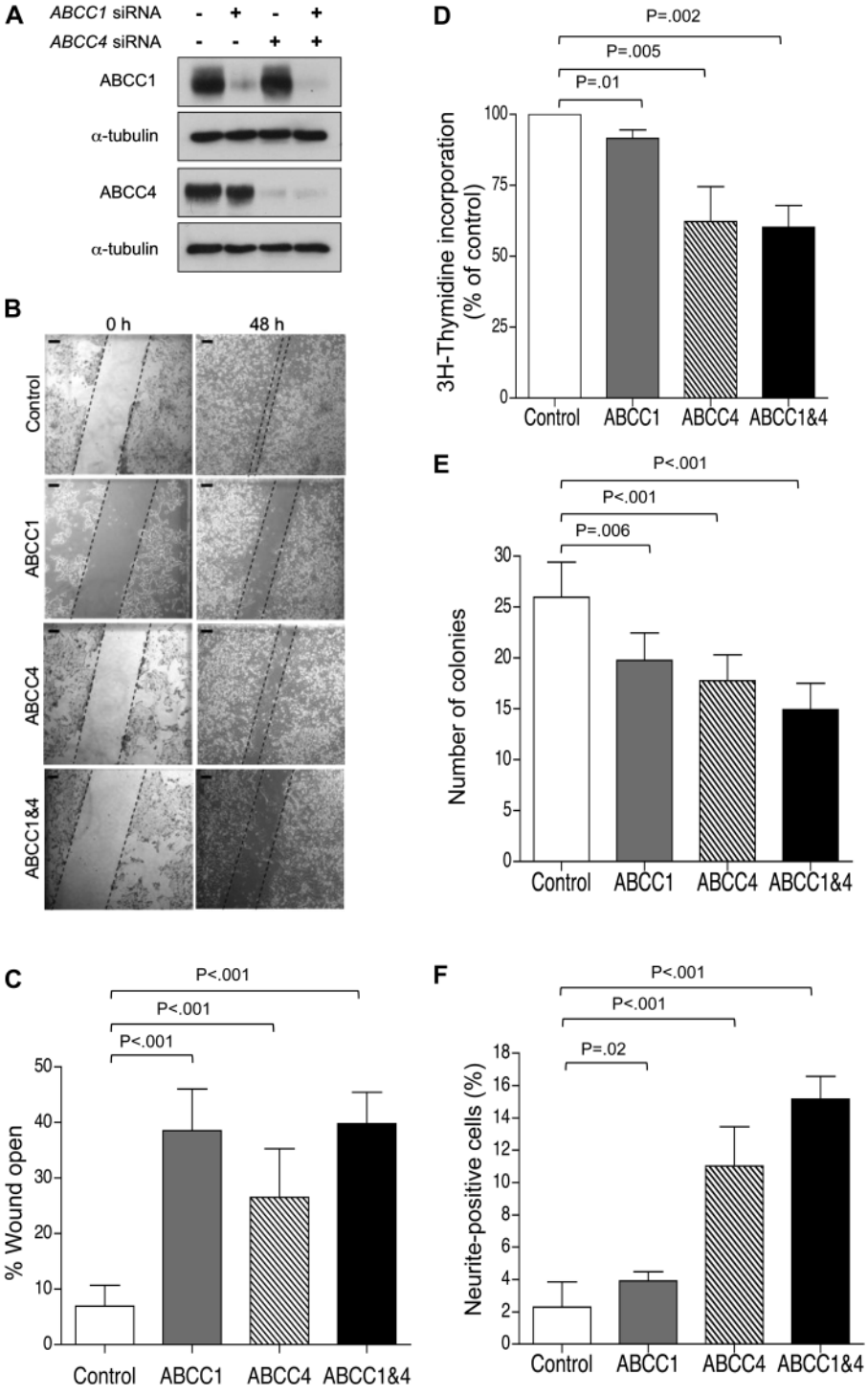

Figure 2. Impact of *ABCC1* and *ABCC4* suppression in BE(2)-C human neuroblastoma cells. **A**) Western blot analysis of ABCC1 and ABCC4 protein expression following exposure of BE(2)-C cells to *ABCC1*- and *ABCC4*-specific siRNA molecules, alone or in combination, or to control siRNA (lane 1). **B**) Representative images of wound closure assay; Scale bar = 125 μm. **C**) Quantification demonstrating impaired motility of BE(2)-C cells depleted of ABCC1, ABCC4, or both, as measured by wound closure assay for 48 hours. **D**) ^{3}H-thymidine incorporation assay in BE(2)-C cells depleted of ABCC1, ABCC4, or both. **E**) Clonogenic capacity of BE(2)-C cells upon depletion of ABCC1 and ABCC4 was assayed after 10 days. **F**) Neurite extension in BE(2)-C cells upon depletion of ABCC1 and ABCC4. In panels (**C**), (**E**), and (**F**), *P* values were derived from two-sided Student *t* test vs control, whereas one-sample *t* test (H_0, μ = 100%) was used in panel (**D**). Means are derived from at least three independent experiments. **Error bars** represent 95% confidence intervals. ABCC = *ATP-binding cassette, subfamily C*; siRNA = short interfering RNA.

7.0 ± 3.5, $P < .001$, two-sided Student *t* test, four independent experiments, Figure 2, C). Combined suppression of ABCC1 and ABCC4 in BE(2)-C cells had no further impact on the magnitude of effect for any of these properties (Figure 2, B–F).

Consistent with a role for ABCC1 in cell motility, *MYCN* non-amplified SH-SY5Y neuroblastoma cells, which have relatively low levels of MYCN and ABCC1 (29,30), displayed considerably enhanced migratory ability when expressing high levels of exogenous ABCC1 in two independent clones: ABCC1 D5 wt and ABCC1 H7 wt (mean % of wound open ± 95% CI: ABCC1 D5 wt, 8.3 ± 5.3 or ABCC1 H7 wt, 13.3 ± 0.4 vs empty vector, 59.9 ± 9.6, $P < .001$, one-way ANOVA and two-sided *t* test, three independent experiments, Figure 3, A–C, Supplementary Figure 1, available online). ABCC1 transporter activity is necessary for the observed effects on cell motility, because forced expression of catalytically inactive ABCC1 (ABCC1-D1454N clone B4 or ABCC1-DE1454LL clone B7) had no impact on cell motility (mean % of wound open ± 95% CI: ABCC1 B4, 49.6 ± 4.5 vs empty vector, 59.9 ± 9.6, $P = .08$; ABCC1 B7, 55.6 ± 9.0 vs empty vector, 59.9 ± 9.6, $P = .54$, one-way ANOVA and two-sided *t* test, three independent

experiments; Figure 3, C). High-level expression of ABCC1 in these cells also enhanced colony-forming ability (mean number of colonies ± 95% CI: ABCC1 D5 wt, 97.6 ± 21.8 or ABCC1 H7 wt, 97.0 ± 18.0 vs empty vector, 73.9 ± 4.3, $P = .03$, one-way ANOVA and two-sided *t* test, four independent experiments; Figure 3, D). This effect was completely abrogated in cells overexpressing the mutant ABCC1 carrying a single amino acid change in the ABC domain (D1454N) or the catalytically inactive double mutant of ABCC1 (DE1454LL) (mean number of colonies ± 95% CI: ABCC1 B4, 74.8 ± 1.6 vs empty vector, 73.9 ± 4.3, $P = .96$; ABCC1 B7, 73.5 ± 5.9 vs empty vector, 73.9 ± 4.3, $P = .88$; one-way ANOVA and two-sided *t* test, four independent experiments; Figure 3, D). Overexpression of ABCC1 did not affect BrdU incorporation in SH-SY5Y cells (mean % of empty vector ± 95% CI: ABCC1 D5 wt, 96.5 ± 12.7; ABCC1 H7 wt, 93.7 ± 11.8, $P = .68$, one-way ANOVA, three independent experiments; Supplementary Figure 5, A, available online).

Next, we examined the impact of genetic or pharmacological suppression of ABCC1 in the *MYCN* nonamplified neuroblastoma cell line, SH-EP. Again, siRNA-mediated ABCC1 depletion impaired motility (mean % wound open ± 95% CI: ABCC1, 22.7 ± 2.4 vs control, 7.8 ± 4.1, $P = .01$, two-sided Student *t* test, three independent experiments; Figure 3, G) and colony-forming ability (mean number of colonies ± 95% CI: ABCC1, 48.5 ± 1.0 vs control, 60.0 ± 2.0, $P = .01$, two-sided Student *t* test, two independent experiments, each with two internal replicates; Figure 3, H) of SH-EP cells, whereas the relatively minor effect on thymidine incorporation observed in BE(2)-C cells was not apparent in SH-EP cells (mean % of control ± 95% CI: ABCC1, 98.4 ± 15.7, $P = .86$, one-sample Student *t* test, three independent experiments; Supplementary Figure 5, B, available online). Inhibition of ABCC1 by Reversan had even more pronounced effects, in terms of reduced wound closure (mean % wound open ± 95% CI: Reversan, 25.0 ± 11.0 vs DMSO, 4.3 ± 1.8, $P = .01$, two-sided Student *t* test, three independent experiments; Figure 3, I and J) and colony-forming ability (mean number of colonies ± 95% CI: Reversan, 58.7 ± 12.3 vs DMSO, 124.7 ± 24.7, $P = .01$, two-sided Student *t* test, three independent experiments, Figure 3, K), than siRNA-mediated ABCC1 suppression, and also in terms of decreased thymidine incorporation (mean % of DMSO control ± 95% CI: Reversan, 65.0 ± 12.9, $P = .033$, one-sample Student *t* test, three independent experiments; Supplementary Figure 5, C, available online). In addition to a reduction in colony number, inhibition of ABCC1 by Reversan also resulted in an effect on colony size, whereby a greater proportion of large (>300 cells) colonies were noted in the controls compared with colonies arising from Reversan-treated SH-EP cells (mean number of large colonies ± 95% CI: DMSO, 99 ± 29.4 vs Reversan, 33 ± 7.25, $P = .01$, two-sided Student *t* test, three independent experiments; Supplementary Figure 5, D, available online). Thus, modulation of ABCC1 by siRNA-mediated suppression, forced expression, or pharmacological inhibition, consistently affected cell motility and clonogenicity in three different neuroblastoma cell lines.

The phenotypic changes observed upon depletion of ABCC4 in BE(2)-C cells using SMARTpool siRNA, involving enhancement of neurite extension and accompanied by decreased thymidine incorporation and colony formation, were investigated further by targeting ABCC4 with individual siRNA duplexes and by examining the effect of ABCC4 suppression in an independent cell line SH-SY5Y. Of the four SMARTpool component duplexes (designated duplex 1 through 4), only duplex 1 was found to effectively suppress ABCC4 expression (Supplementary Figure 6, A, available online; data not shown). However, efficient suppression of ABCC4 expression was also achieved using an independent sequence targeting ABCC4 (18) (Supplementary Figure 6, A, available online, ABCC4.5). Using either of these sequences to target ABCC4 in BE(2)-C cells, even more pronounced effects on neurite extension (mean % neurite-positive cells ± 95% CI: ABCC4.1, 17.8 ± 4.9 or ABCC4.5, 27.3 ± 3.3 vs control, 2.6 ± 1.6, $P < .001$, one-way ANOVA and two-sided *t* test, three independent experiments; Supplementary Figure 6, B, available online), thymidine incorporation (mean % of control ± 95% CI: ABCC4.1, 55.0 ± 11.4, $P = .004$; ABCC4.5, 45.9 ± 20.6, $P = .014$, one-way ANOVA and one-sample *t* test, three independent experiments; Supplementary Figure 6, C, available online), and colony formation (mean number of colonies ± 95% CI: ABCC4.1, 27.6 ± 3.9 or ABCC4.5, 30.8 ± 9.6 vs control, 54.8 ± 7.6, $P < .001$, one-way ANOVA and two-sided *t* test, three independent experiments; Supplementary Figure 6, D, available online) than had been evident with the SMARTpool siRNA were observed. Upon depletion of ABCC4 in SH-SY5Y cells using SMARTpool siRNA (Figure 4, A), the results obtained were entirely consistent with those observed in the BE(2)-C cell line. Thus, ABCC4 suppression resulted in a substantial increase in the proportion of cells extending neuritic processes, despite the high basal level of neurites for this cell line (mean % neurite-positive cells ± 95% CI: ABCC4, 39.5 ± 6.7 vs control, 24.0 ± 4.5, $P = .01$, two-sided Student *t* test, three independent experiments; Figure 4, B). This increased morphological differentiation was accompanied by statistically significantly reduced thymidine incorporation (mean % of control ± 95% CI: ABCC4, 68.1 ± 13.1, $P = .02$, one-sample Student *t* test, three independent experiments; Figure 4,C) and colony-forming ability (mean number of colonies ± 95% CI: ABCC4, 98.1 ± 16.3 vs control, 143.2 ± 10.8, $P = .004$, two-sided Student *t* test, three independent experiments; Figure 4, D). Finally, we examined the effect of pharmacological inhibition of ABCC4 on the behavior of BE(2)-C cells. Although there is a current lack of potent and specific ABCC4 inhibitors, we have identified, through chemical small-molecule library screening, a number of compounds that sensitize ABCC4-overexpressing cells to the well-characterized ABCC4 substrate, 6-mercaptopurine (6-MP), and that enhance ^{14}C-6-MP accumulation in these cells. Importantly, among these compounds, we have identified at least two that substantially reduce the growth of BE(2)-C cells and enhance their neurite formation (data not shown), thus closely recapitulating the effects of siRNA-mediated ABCC4 depletion.

Together, these data indicate that in the absence of chemotherapeutic agents, modulation of ABCC1 or ABCC4 can influence multiple neuroblastoma cell characteristics relevant to tumor progression.

ABCC Family Gene Expression and Outcome in Primary Neuroblastoma

In addition to ABCC1, other members of the C branch of the ABC transporter family expel both cytotoxic drugs and a range of

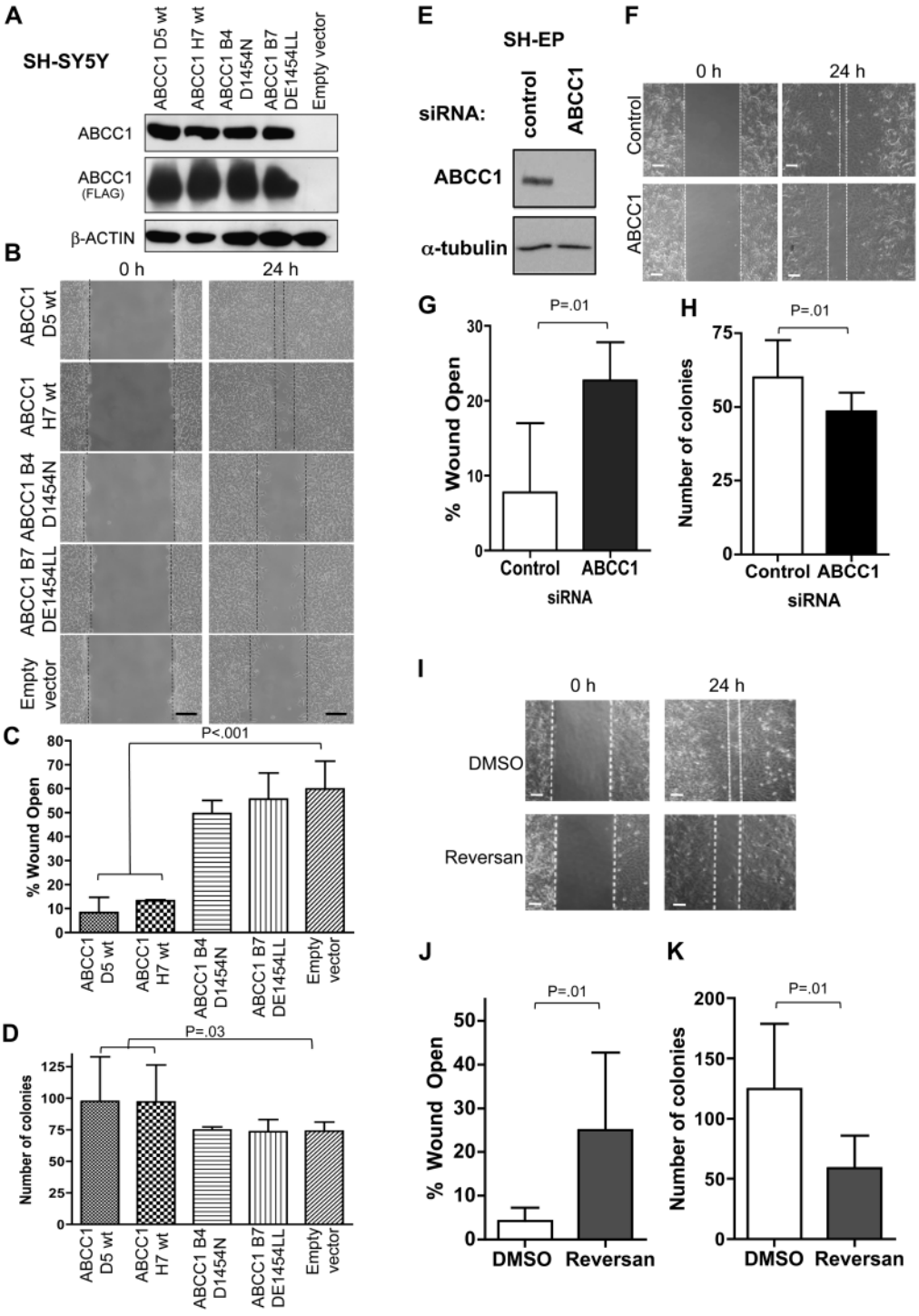

Figure 3. Impact of *ABCC1* modulation in SH-SY5Y and SH-EP neuroblastoma cells. **A**) Western blot analysis of ABCC1 protein expression following stable transduction of SH-SY5Y cells with either empty vector, wild-type (wt) ABCC1 (clones D5, H7), ABCC1 D1454N single mutant (clone B4), or ABCC1 DD1454LL double mutant (clone B7) constructs. Refer to Supplementary Figure 1 (available online) for verification of membrane-localized transporter expression. **B**) Representative images of wound closure assay; Scale bar = 125 μm. **C**) Expression of ABCC1-wt and motility of SH-SY5Y cells, as measured by wound closure assay for 24 hours, compared with catalytically inactive mutants. **D**) Quantification of colony-forming assay upon expression of ABCC1-wt or catalytically inactive mutants in SH-SY5Y cells. In panels (**C**) and (**D**), one-way analysis of variance followed by two-sided *t* tests vs control were used to generate *P* values. **E**) Western blot analysis of ABCC1 protein expression following exposure of SH-EP cells to *ABCC1*-specific siRNA, or to control siRNA. **F**) Representative images of wound closure assay; Scale bar = 125 μm. **G**) Quantification indicating impaired wound closure ability upon ABCC1 suppression. **H**) ABCC1 depletion and impaired colony-forming ability. **I**, **J**) Wound closure and **K**) colony-forming abilities of SH-EP cells upon pharmacological inhibition of ABCC1 using 5 μM Reversan. Means displayed in all panels are derived from at least three independent experiments except for the clonogenicity assay of siRNA-transfected SH-EP cells (**H**), which was derived from two independent experiments, each with two internal replicates. In panels (**G**), (**J**), and (**K**), *P* values were derived from the two-sided Student *t* test vs control. **Error bars** represent 95% confidence intervals. ABCC1 = ATP-binding cassette, subfamily C, member 1; DMSO, dimethyl sulfoxide; siRNA = short interfering RNA.

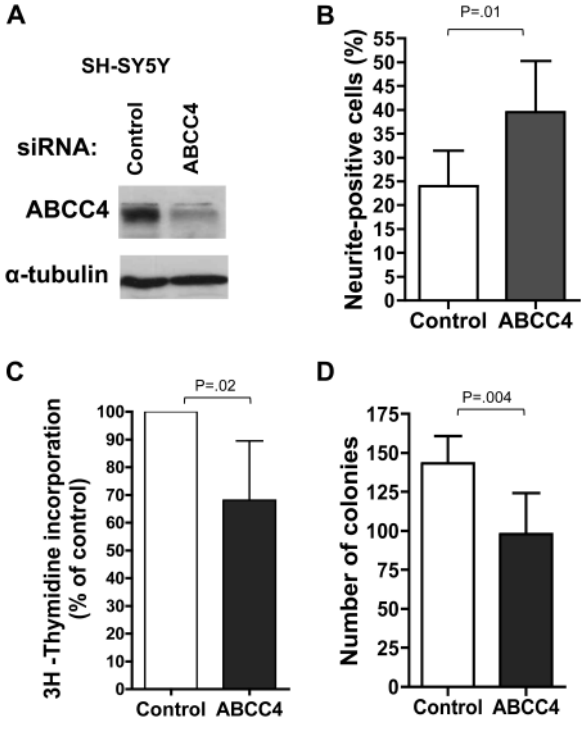

Figure 4. Impact of *ABCC4* suppression in SH-SY5Y neuroblastoma cells. **A**) Western blot analysis of ABCC4 protein expression following exposure of SH-SY5Y cells to *ABCC4*-specific SMARTpool siRNA, or to control siRNA. **B**) Enhanced neurite extension in SH-SY5Y cells upon depletion of ABCC4. **C**) ^{3}H-thymidine incorporation in SH-SY5Y cells depleted of ABCC4. **D**) Clonogenic capacity upon depletion of ABCC4 was assayed after 12 days. In panel (**B**) and (**D**), *P* values were derived from two-sided Student *t* test vs control, whereas one-sample *t* test was used in panel (**C**) (H_0, μ = 100%). Means are derived from three replicate experiments and **error bars** represent 95% confidence intervals. ABCC4 = ATP-binding cassette, subfamily C, member 4; siRNA = short interfering RNA.

endogenous substrates that are capable of influencing tumor behavior [reviewed in (11,31,32)]. Having established that ABCC1 can affect the behavior of neuroblastoma cells both in vitro and in vivo and that ABCC4 can also influence neuroblastoma cell characteristics, we assessed whether the expression of other ABCC family members was associated with clinical outcome in this disease and whether their effects might be independent of cytotoxic drug efflux. We therefore analyzed the expression of the remaining ABCC family members (including ABCC4, which had previously been investigated only in a small retrospective study) in 209 prospectively accrued primary neuroblastomas (refer to Materials and Methods and Supplementary Figure 3, available online, for cohort description). Initial examination of *ABCC* gene family members revealed that expression levels of *ABCC6*, *ABCC7*, and *ABCC10–12* were either extremely low or undetectable in a representative subset of neuroblastoma samples. These genes were not examined further. Expression levels of the remaining genes, *ABCC2-5* and *ABCC8-9*, were determined for the entire neuroblastoma cohort by real-time polymerase chain reaction.

Like *ABCC1*, which we previously showed to be highly expressed in tumors with *MYCN* amplification (5,6), we found statistically significantly higher levels of *ABCC4* expression in neuroblastomas with *MYCN* amplification (n = 23), compared with those without *MYCN* amplification (n = 184) (mean ΔΔCt ± 95% CI: MYCN-amplified, 962 ± 495.9 vs MYCN nonamplified, 96 ± 21.6, $P < .001$, two-sided Student *t* test). *ABCC4* expression was also associated with advanced tumor stage (Table 1; $P = .03$). We also observed a strong inverse association between *ABCC3* expression and advanced tumor stage (Table 1; $P = .003$) and also older age at diagnosis (Table 1; $P < .001$). Expression of *ABCC8* and *ABCC9* was associated with *MYCN* amplification (mean ΔΔCt *ABCC8* ± 95% CI: MYCN-amplified, 53 ± 33.3 vs MYCN nonamplified, 29 ± 6.9, $P = .04$, and mean ΔΔCt *ABCC9* ± 95% CI: MYCN-amplified, 5.2 ± 7.3 vs MYCN nonamplified, 3.9 ± 0.33, $P = .02$, two-sided Student *t* tests). Whereas expression of *ABCC2*, *ABCC5*, and *ABCC9* was associated with older age at diagnosis (Supplementary Table 2, available online), there were no associations between expression of *ABCC2*, *ABCC5*, or *ABCC8-9* and tumor stage (Supplementary Table 2, available online).

As previously described for this cohort, *ABCC1* expression was found to be strongly associated with outcome following dichotomization

Table 1. Clinical and molecular characteristics of neuroblastoma patient tumors*

	No. of patients							
	***MYCN* amplification**		***ABCC1* expression**		***ABCC3* expression**		***ABCC4* expression**	
Clinical characteristic	**Present**	**Absent**	**High**	**Low**	**High**	**Low**	**High**	**Low**
Age†								
<1 y	3	93	12	84	87	8	9	87
>1 y	20	91	8	104	67	45	11	101
Tumor stage‡								
Favorable	1	105	8	98	87	18	6	100
Unfavorable	22	65	12	76	56	32	14	74

* Two hundred and nine study patients; Categories are overlapping. *MYCN* amplification was considered absent if there were nine or fewer FISH signals for *MYCN* per tumor cell and present if there were more than nine signals. Status of two case patients was unknown. For *ABCC1* and *ABCC4*, the level of expression was considered high or low in relation to the upper decile of ΔΔCt values for all tumors analyzed. For *ABCC3*, the level of expression was considered high or low in relation to the lower quartile of ΔΔCt values for all tumors analyzed. ΔΔCt method is the comparative threshold cycle method of transcript quantification. *ABCC = ATP-binding cassette, subfamily C*; FISH = Fluorescence in situ hybridization; *MYCN = v-myc myelocytomatosis viral related oncogene, neuroblastoma derived.*

† Age (categorized as <1 or >1 year at diagnosis) was statistically significantly associated with *MYCN* amplification ($P < .001$) and with *ABCC*3 expression ($P < .001$) (Two-sided Fisher exact tests). Age was unknown for one patient.

‡ Tumor stage was categorized as favorable (INSS stages 1, 2A/2B, or 4S) or unfavorable (INSS stages 3 or 4) and was unknown in 15 case patients. Tumor stage was statistically significantly associated with *MYCN* amplification ($P < .001$), *ABCC3* expression ($P = .003$), and *ABCC4* expression ($P = .03$) (Two-sided Fisher's exact tests). INSS = International Neuroblastoma Staging System.

around the upper decile (5). Using this same cut point, high *ABCC4* expression was also strongly associated with reduced event-free survival (HR = 4.7, 95% CI = 2.5 to 8.9; $P < .001$) and overall survival (HR = 5.4, 95% CI = 2.8 to 10.4; $P < .001$; Table 2 and Supplementary Figure 7, A, available online), consistent with earlier findings in a smaller separate cohort (12). Again, none of the patients in this study were treated with any cytotoxic drugs that are substrates of ABCC4. Similar results were obtained when the data were dichotomized using the mean or upper quartile as cut points (data not shown). In contrast, low levels, rather than high levels, of *ABCC3* expression were strongly associated with reduced event-free survival (HR = 2.4, 95% CI = 1.4 to 4.2; $P = .001$) and reduced overall survival (HR = 2.4, 95% CI = 1.3 to 4.3; $P = .003$; Table 2 and Supplementary Figure 7, D, available online), with 23 of 53 patients with low *ABCC3* expression experiencing recurrence or death compared with 31 of 155 patients with high *ABCC3*. This result remained statistically significant whether the upper quartile, median, or lower quartile was used for dichotomization, with the lower quartile maximally differentiating outcome of patients. No other *ABCC* genes predicted outcome, regardless of the cut point used (Supplementary Table 3, available online).

ABCC1 expression was highly prognostic in subsets of patients expected to have either particularly poor or particularly good outcome (5). Extending this observation, in patients with advanced disease (stages 3 and 4), high *ABCC4* or low *ABCC3* expression was associated with statistically significantly worse outcome (% 5-year event-free survival ± 95% CI: high *ABCC4*, 21 ± 43.1 vs low *ABCC4*, 54 ± 23.5, $P < .001$ and % 5-year event-free survival ± 95% CI: low *ABCC3*, 34 ± 33.3 vs high *ABCC3*, 57 ± 25.5, $P = .03$; Supplementary Figure 7, B and E, available online). Similarly, for patients without *MYCN* amplification, low-level *ABCC4* or high-level *ABCC3* expression was associated with better outcome compared with patients having high *ABCC4* or low *ABCC3* expression (% 5-year event-free survival ± 95% CI: high *ABCC4*, 53 ± 66.6 vs low *ABCC4*, 80 ± 11.8, $P = .022$ and % 5-year event-free survival: low *ABCC3*, 63 ± 27.4 vs high *ABCC3*, 84 ± 13.7, $P = .0016$; Supplementary Figure 7, C and F, available online).

In testing for the independent prognostic significance of *ABCC1*, *ABCC3*, and *ABCC4* gene expression in a model with tumor stage, age, and *MYCN* amplification, only stage (HR of recurrence or death = 4.5, 95% CI = 2.1 to 9.9; $P < .001$) and the three *ABCC* genes (HR, high *ABCC1* = 2.3, 95% CI = 1 to 5; $P = .04$; low *ABCC3* = 2.3, 95% CI = 1.2 to 4.4; $P = .01$; high *ABCC4* = 3.1, 95% CI = 1.2 to 7.7, $P = .02$) remained associated with event-free survival (Table 2). Age and *MYCN* amplification were not independently statistically significant in this model. The only factors that retained independent prognostic significance for overall survival were tumor stage (HR of death = 9.5, 95% CI = 3.2 to 27.6; $P < .001$) and *ABCC4* expression (HR of death = 3.2, 95% CI = 1.2 to 8.3; $P = .02$).

Given the strong association between altered expression of these three transporters and clinical outcome, we examined the prognostic value of their combined expression pattern. In this analysis, there were eight possible combinations based on high or low expression of the three genes. These eight combinations were descriptively compared with Kaplan–Meier curves, and clusters were recategorized into groups, such that curves not statistically significantly different from one another were included in the same group (Figure 5, A). These statistical groupings were subsequently found to accurately reflect biological risk associated with *ABCC* gene expression. Group A included only those patients whose tumors displayed low levels of *ABCC1* and *ABCC4* and high levels of *ABCC3*, reflecting "favorable" *ABCC* gene expression. The 5-year cumulative event-free survival rate of this group was 85% (95% CI = 77% to 90%). Group B consisted of patients whose tumors displayed only one unfavorable risk factor with respect to the three *ABCC* genes analyzed (ie, *ABCC1* high, *ABCC4* high, or *ABCC3* low), and the event-free survival rate of this group was 60% (95% CI = 47% to 71%). Group C was found to comprise patients whose tumors exhibited two or more unfavorable *ABCC* risk factors, and the event-free survival rate of patients in this

Table 2. Univariate and multivariable Cox regression analysis of factors prognostic for outcome in neuroblastoma*

	Event-free survival		Overall survival	
Factor	**HR (95% CI)†**	***P*‡**	**HR(95% CI)**	***P*‡**
Univariate				
High ABCC1 expression (n = 209)	3.8 (2.0 to 7.2)	<.001	3.4 (1.7 to 6.8)	.001
Low ABCC3 expression (n = 208)	2.4 (1.4 to 4.2)	.001	2.4 (1.3 to 4.3)	.003
High ABCC4 expression (n = 209)	4.7 (2.5 to 8.9)	<.001	5.4 (2.8 to 10.4)	<.001
Multivariable (n = 192)§				
High ABCC1 expression	2.3 (1.0 to 5.0)	.04	1.7 (0.7 to 3.9)	.21
Low ABCC3 expression	2.3 (1.2 to 4.4)	.01	1.9 (1.0 to 3.8)	.06
High ABCC4 expression	3.1 (1.2 to 7.7)	.02	3.2 (1.2 to 8.3)	.02
Advanced tumor stage	4.5 (2.1 to 9.9)	<.001	9.5 (3.2 to 27.6)	<.001
Older age	1.8 (0.8 to 3.8)	.14	2.1 (0.9 to 4.9)	.10
MYCN amplification	1.02 (0.5 to 2.3)	.96	1.1 (0.5 to 2.6)	.75

* *MYCN* amplification was considered absent if there were nine or fewer FISH signals for *MYCN* per tumor cell and present if there were more than nine signals. Status of two case patients was unknown. For *ABCC1* and *ABCC4*, the level of expression was considered high or low in relation to the upper decile of ΔΔCt values for all tumors analyzed. For *ABCC3*, the level of expression was considered high or low in relation to the lower quartile of ΔΔCt values for all tumors analyzed. ΔΔCt method is the comparative threshold cycle method of transcript quantification. *ABCC = ATP-binding cassette, subfamily C*; FISH = Fluorescence *in situ* hybridization; *MYCN = v-myc myelocytomatosis viral related oncogene, neuroblastoma derived.*

† Hazard ratios were calculated as the antilogs of the regression coefficients in the proportional hazards regression.

‡ Univariate: log-rank test; Multivariable: Cox model.

§ Multivariable analysis was performed following inclusion of all listed prognostic factors into the Cox regression model.

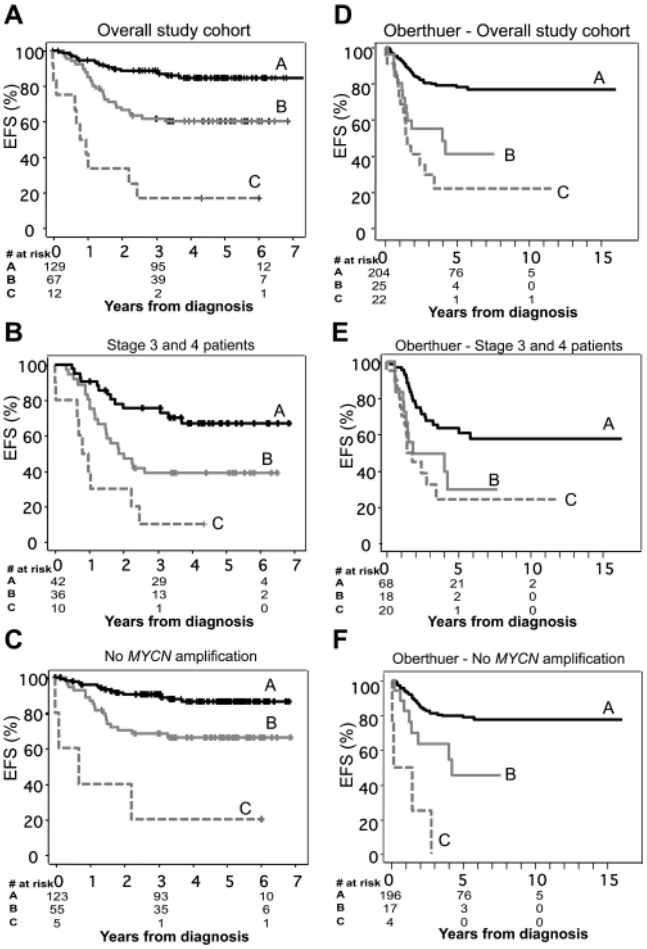

Figure 5. Prognostic significance of *ABCC* gene expression in neuroblastoma. **A**) Combined expression of the *ABCC1*, *ABCC3* and *ABCC4* genes and cumulative event-free survival (EFS) in 209 patients with neuroblastoma. Patients were categorized into eight clusters on the basis of their combined *ABCC1*, *ABCC3*, and *ABCC4* expression pattern. Kaplan–Meier survival analysis of these clusters revealed three statistically distinct groupings (Groups A, B, and C), which were associated with the risk of relapse associated with individual *ABCC* gene expression. Group A included only those patients whose tumors displayed low levels of *ABCC1* and *ABCC4* and high levels of *ABCC3*, reflecting "favorable" *ABCC* gene expression. Group B consisted of patients whose tumors displayed only one unfavorable risk factor with respect to the three *ABCC* genes analyzed (ie, *ABCC1* high, *ABCC4* high, or *ABCC3* low), and Group C comprised patients whose tumors exhibited two or more unfavorable *ABCC* risk factors. Similar associations between combined *ABCC* gene expression and increasingly poor outcome were also observed in subgroups of patients (**B**) with stage 3 or 4 disease or (**C**) whose tumors lacked *MYCN* amplification. **D)** Combined expression of the *ABCC1*, *ABCC3*, and *ABCC4* genes and cumulative EFS in 251 neuroblastoma patient samples analyzed by Oberthuer et al. (27). Patients in the Oberthuer et al. (27) cohort were categorized into eight groups as described for panel (**A**) above. These groupings were also strongly predictive of EFS in subgroups of patients (**E**) with unfavorable (stages 3 and 4) disease or (**F**) with non–*MYCN*-amplified disease. At 0, 3, and 6 years from diagnosis [Panels (**A**), (**B**), and (**C**)], or 0, 5, and 10 years from diagnosis [Panels (**D**), (**E**), and (**F**)], the number of patients at risk of relapse are shown. *ABCC = ATP-binding cassette, subfamily C*; *MYCN = v-myc myelocytomatosis viral related oncogene, neuroblastoma derived.*

group was 17% (95% CI = 3% to 41%). The combined expression of *ABCC1*, *ABCC3*, and *ABCC4* was associated with patients having an adverse event, such that of the 12 patients with the "poor prognosis" expression pattern, 10 experienced recurrence or death. Patients in this group were 12 times more likely to have an adverse event (HR of recurrence or death = 12.3; 95% CI = 6 to 27; $P < .001$). Combined *ABCC* gene expression was also analyzed in subgroups of patients with unfavorable (stages 3 and 4) disease (Figure 5, B) or without *MYCN* amplification (Figure 5, C) and found for each case to be highly prognostic of outcome. The risk of an adverse event for Group C patients was high in both subgroups with a hazard ratio of 6.4 (95% CI = 3 to 15; $P < .001$) for patients with stage 3 or 4 tumors and 13.9 (95% CI = 5 to 42; $P < .001$) for patients without *MYCN* amplification.

Multivariable analysis of combined expression of the *ABCC1*, *ABCC3*, and *ABCC4* genes, including tumor stage, age, and *MYCN* amplification as variables, revealed stage and unfavorable expression of one (Group B) or more (Group C) *ABCC* genes as independent indicators of event-free survival, with the hazard ratio for an adverse event in Group B being 2.05 (95% CI = 1 to 4; $P = .033$) and in Group C being 5.02 (95% CI = 2 to 14; $P = .001$).

Validation of Prognostic Significance of *ABCC1, ABCC3,* and *ABCC4* in an Independent Dataset

To verify the prognostic significance of *ABCC* gene expression in an independent cohort, we analyzed a publicly available dataset from Oberthuer et al. (27) containing clinical, pathological, and gene expression data for 251 primary neuroblastoma tumors. From this dataset, normalized expression data generated by custom oligonucleotide microarray hybridization were extracted for *ABCC1*, *ABCC3*, and *ABCC4* and the association with clinical outcome examined. Again, high expression of either *ABCC1* (HR of recurrence or death = 4.7; 95% CI = 2.7 to 8.1; $P < .001$) or *ABCC4* (HR = 3.95; 95% CI = 2.3 to 6.8; $P < .001$) was strongly associated with reduced event-free survival, as was low expression of *ABCC3* (HR = 3.35; 95% CI = 1.9 to 5.95; $P < .001$). Furthermore, when patients were grouped according to the combined expression pattern of *ABCC1*, *ABCC3*, and *ABCC4* as described above, these groupings were again found to distinguish good, intermediate, and poor patient outcome (Figure 5, D). Five-year cumulative event-free survival was 77% (95% CI = 70% to 83%) in Group A, which included only those patients whose tumors displayed low levels of *ABCC1* and *ABCC4* and high levels of *ABCC3* reflecting favorable *ABCC* gene expression, whereas event-free survival in Group B was 41% (95% CI = 19% to 63%) and in Group C only 22% (95% CI = 2.4 to 41%; $P < .001$). These groupings were also strongly predictive of event-free survival in subgroups of patients with unfavorable (stages 3 and 4) disease (Group A = 57% [95% CI = 44% to 71%], Group B = 30% [95% CI = 4.2% to 55%], Group C = 24% [95% CI = 2.9% to 45%], $P < .001$; Figure 5, E) or with non–*MYCN*-amplified disease (Group A = 77% [95% CI = 71% to 84%], Group B = 45% [95% CI = 18% to 72%], Group C = 0% [95% CI = 0% to 0%], $P < .001$; Figure 5, F). Of the other ABCC genes examined, expression data for *ABCC2* and *ABCC8* were also available in this dataset. Consistent with our study, neither of these genes was statistically significantly associated with patient outcome.

ABCC3 Expression and Neuroblastoma Cell Characteristics

Surprisingly, the analysis of ABCC gene expression in two independent cohorts of neuroblastoma patients demonstrated a

powerful independent association between low levels of *ABCC3* expression and clinical outcome. Although patients in both cohorts were treated with etoposide (5,27,33), an ABCC3 substrate, only an association between high-level expression of an ABCC family member and poor clinical outcome could be explained in terms of enhanced drug transport mediating chemotherapeutic drug resistance and hence clinical outcome.

To investigate the significance of low *ABCC3* expression in neuroblastoma, BE(2)-C cells, which have extremely low endogenous levels of ABCC3, were transduced to constitutively express ABCC3. Stable clones expressing ABCC3 (Figure 6, A) displayed substantially impaired cellular migratory activity, as measured by wound closure ability (mean % of wound open ± 95% CI: ABCC3 B12 wt, 55.0 ± 9.0 or ABCC3 A12 wt, 50.5 ± 4.5 vs empty vector, 1.5 ± 2.0, $P < .001$, one-way ANOVA and two-sided *t* test, three independent experiments; Figure 6, B and C), and reduced colony-forming capacity (mean number of colonies ± 95% CI: ABCC3 B12 wt, 75.1 ± 2.35 or ABCC3 A12 wt, 73.9 ± 2.7 vs empty vector, 90.9 ± 9.4, $P = .03$, one-way ANOVA and two-sided *t* test, three independent experiments; Figure 6, C), although no statistically significant impact on cell proliferation was observed (mean % of empty vector ± 95% CI: ABCC3 B12 wt, 83.4 ± 9.0; ABCC3 A12 wt, 87.6 ± 9.6, $P = .22$, one-way ANOVA, three independent experiments, Figure 6, E). Similar results were obtained upon stable expression of ABCC3 in mass-transfected pools (Supplementary Figure 8, available online). ABCC3 transport activity is necessary for the observed effects on cell motility and clonogenicity, because the wound closure and colony-forming ability of cells expressing catalytically inactive ABCC3 (ABCC3-V1322F) were indistinguishable from cells transfected with empty vector (mean % of wound open ± 95% CI: ABCC3 C4, 5.4 ± 4.3 vs ABCC3 D1, 3.0 ± 2.4 vs empty vector, 1.5 ± 2.0, $P = .34$, one-way ANOVA, three independent experiments; Figure 6, C and mean numberof colonies ± 95% CI: ABCC3 C4, 91.1 ± 6.5 vs ABCC3 D1, 92.0 ± 7.4 vs empty vector, 90.9 ± 9.4, $P = .98$, one-way ANOVA, three independent experiments; Figure 6, D).

Collectively, these data clearly indicate that ABCC1, ABCC3, and ABCC4 have the ability to affect multiple aspects of tumor cell

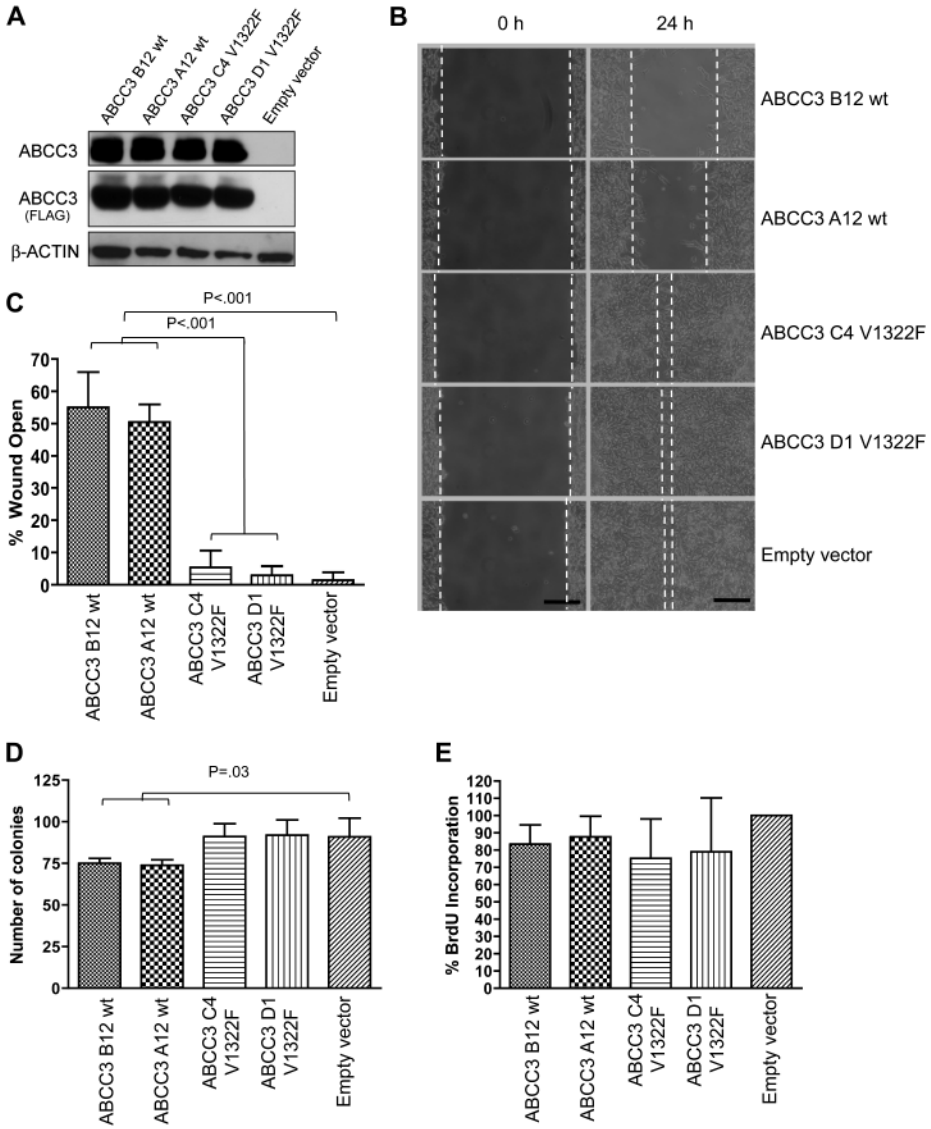

Figure 6. Impact of *ABCC3* gene expression on human BE(2)-C neuroblastoma cell characteristics. **A**) Western blot analysis of ABCC3 protein expression following stable transduction of BE(2)-C cells with either empty vector, wild-type (wt) ABCC3 (clones A12, B12) or ABCC3 V1322F mutant (clones C4, D1) constructs. Refer to Supplementary Figure 2 (available online) for verification of membrane-localized transporter expression. **B**) Representative images of wound closure assay; Scale bar, 125 μm. **C**) Expression of ABCC3-wt and impaired motility of BE(2)-C cells, as measured by wound closure assay for 24 hours, compared with catalytically inactive mutant. **D**) Colony-forming assay and **E**) Bromodeoxyuridine (BrdU) incorporation upon expression of ABCC3-wt or catalytically inactive mutant in BE(2)-C cells. One-way analysis of variance followed by two-sided *t* tests vs control were used to generate *P* values. Means are derived from three replicate experiments and **error bars** represent 95% confidence intervals. ABCC3 = ATP-binding cassette, subfamily C, member 3.

phenotype, independent of any role in cytotoxic drug efflux and drug resistance.

Discussion

Although several studies suggest that ABC drug transporters contribute to tumor progression independent of their drug efflux capabilities [reviewed in (11)], the evidence has remained essentially correlational to date. The current study provides direct genetic evidence that an ABC transporter, ABCC1, can contribute to tumor development in a mouse cancer model. Furthermore, this study demonstrates that high-level expression of *ABCC4* and low-level expression of *ABCC3* are both highly associated with clinical outcome in patients with neuroblastoma, a result not accounted for by the cytotoxic drug efflux capacities of either protein. The combined expression of ABCC1, ABCC3, and ABCC4 stratified patients into groups having excellent, intermediate, or poor outcome, and this combination of factors is one of the most powerful independent prognostic markers yet, to our knowledge, identified for this disease. Finally, this study demonstrates that each of these transporters affects multiple characteristics of cultured neuroblastoma cells, providing initial insights into the physiological function of these transporters beyond drug efflux.

The ABCC branch of the ABC transporter superfamily contains several transporters known to confer cellular resistance to clinically important chemotherapeutic agents (9). The best characterized of these, ABCC1, transports several classes of chemotherapeutic drugs commonly used in the treatment of neuroblastoma including *Vinca* alkaloids, epipodophyllotoxins, and anthracyclines. We found that pharmacological inhibition of ABCC1 using Reversan, or deletion of one *Abcc1* allele, delays tumor formation in the *hMYCN* transgenic mouse model of neuroblastoma in the absence of antineoplastic agents. Consistent with this observation, siRNA-mediated depletion of ABCC1 or inhibition of ABCC1 with Reversan in neuroblastoma cell lines impaired cell motility and clonogenic capacity, also in the absence of chemotherapeutic agents. These results reinforce earlier observations in which introduction of antisense mRNA to *ABCC1* into neuroblastoma cells resulted in reduced cell growth and increased apoptosis in cell culture or cell line xenograft models (29,34). Conversely, forced high-level expression of ABCC1 enhanced cell migratory ability and clonogenic ability, with these effects shown to be dependent on the ATP-driven efflux capacity of ABCC1. Together, these results provide compelling evidence for a role for ABCC1-mediated efflux of endogenous cellular substrates in neuroblastoma biology.

We have now found high *ABCC4* expression to be strongly predictive of poor outcome in three independent cohorts. In contrast to the broad substrate specificity of ABCC1, *ABCC4* overexpression has been shown to confer resistance only to nucleoside analogs and topoisomerase poisons, such as camptothecin, irinotecan, and topotecan (9,35,36), none of which were used to treat the patients within any of these cohorts. In addition, this study identified low, rather than high, expression of *ABCC3* as being predictive of poor outcome, despite the ability of ABCC3 to expel the important neuroblastoma chemotherapeutic, etoposide. Consistent with these observations, siRNA-mediated silencing of *ABCC4* using either SMARTpool siRNA or either of two independent siRNA duplexes in two different neuroblastoma cell lines, led to an increase in morphological differentiation and reduced growth capacity, with these effects being faithfully recapitulated by chemical small molecules that inhibit ABCC4-mediated drug efflux. By comparison, the most prominent phenotype associated with ABCC1 modulation was altered cell motility, with little impact on morphological differentiation. Although depletion of either gene impaired colony-forming ability, suggesting that these proteins may share some functions, ABCC4 modulation had a substantially more pronounced effect on proliferation, as measured by ^{3}H-thymidine or BrdU incorporation, perhaps pointing to distinct mechanisms. Consistent with low-level expression of *ABCC3* being associated with poor clinical outcome in neuroblastoma, overexpression of *ABCC3* led to decreased cell motility and colony formation, with these effects again being shown to be dependent on the catalytic activity of ABCC3 and suggesting involvement of efflux of cellular substrates important to neuroblastoma biology. The finding that forced expression of *ABCC3* mirrored the effects of ABCC1 depletion suggests opposing roles for these proteins in neuroblastoma.

Thus, although high *ABCC1* expression in neuroblastoma can clearly contribute to the chemoresistant behavior of this tumor through enhanced drug efflux (5,10), our data provide compelling evidence for an additional and more direct contribution to tumor growth and progression. The prognostic power of high *ABCC4* expression and low *ABCC3* expression for poor outcome, together with the inability of known cytotoxic drug substrates to account for these associations in the cohorts studied, as well as the impact of modified expression of these genes on neuroblastoma cell phenotypes, all suggest that these transporters may also contribute to neuroblastoma biology and clinical outcome independently of drug efflux. Crossbreeding experiments between MYCN transgenic mice and *Abcc3* and *Abcc4* gene knockout models, paralleling those already undertaken with *Abcc1* knockout mice, are the essential next steps to determine the true biological impact of these two transporters in neuroblastoma development, progression, and treatment response in vivo. These studies are currently underway and will be important in validating these genes as worthwhile therapeutic targets for this disease.

Although the mechanisms underlying these observations are at present unknown, the efflux of endogenous substrates seems to be the most probable. ABCC1 expels a diverse range of physiological substrates including folates, phosphosphingolipids, glutathione, leukotrienes, and glutathione conjugates of steroids, many of which have established roles in tumor development and progression, and the activities of this transporter are important in a range of normal cellular processes such as export of endogenous intermediates and protection from toxic insult [see (11,37) for recent reviews]. Recently, ABCC1 was found to play a role in migration of thyroid carcinoma cells by mediating efflux of the inflammatory mediator sphingosine-1-phosphate (38) and was responsible for mediating the antiapoptotic effects of glucocorticoids in human fibroblasts by promoting sphingosine-1-phosphate efflux (39). Mice lacking ABCC1 display an altered response to inflammatory stimuli, most likely attributable to decreased secretion of the

proinflammatory cytokine leukotriene C4, which has the highest affinity for ABCC1 of any known transporter substrate (40). An association between chronic inflammation and cancer has long been observed, and the products of arachidonic acid metabolism, including leukotrienes and prostaglandins, appear to be involved in both inflammatory processes and cancer cell growth (37,41). Notably, blocking arachidonic acid metabolism through the use of nonsteroidal anti-inflammatory drugs has been shown to inhibit neuroblastoma cell growth both in vitro and in vivo (42). In light of the known physiological roles of ABCC1, it was interesting to observe that the protective effect of deletion of one allele of *Abcc1* in the MYCN transgenic model of neuroblastoma tumorigenesis was not augmented by deletion of the second *Abcc1* allele. This effect could be attributed to compensatory increased expression of, for example, one of the many other ABC transporter genes or else could represent haploinsufficiency, if loss of only one allele was sufficient to bring about the maximal phenotype. However, it is also possible that the effect is associated with the putative role for ABCC1 in dendritic cell homing to lymph nodes, which may in turn play a critical role in tumor surveillance (40,43). This hypothesis deserves further attention because it has implications for the development of clinical strategies for targeted inhibition of ABCC1 and potentially other ABC transporters.

ABCC4 can mediate the low-affinity transport of cyclic-nucleotides (cGMP and cAMP) (44), which are key effectors of G-protein-coupled receptors that regulate multiple aspects of cell growth. In cultured neuroblastoma cells, elevation of cAMP levels leads to decreased growth and increased morphological differentiation (45,46). Alternately, as with ABCC1, in vivo and in vitro models have shown that ABCC4 mediates transport of inflammatory mediators such as prostaglandins, leukotrienes, and conjugated steroids (47–49). This transporter has a major functional role in the efflux of prostaglandin E2 (18), which is known to influence diverse cellular processes involved in inflammation, as well as neoplastic transformation and progression (50,51).

Conversely, the strong association of low *ABCC3* expression with poor clinical outcome suggests that ABCC3 may be transporting an endogenous substrate inhibitory to neuroblastoma growth and metastasis. Consistent with this, *ABCC3* expression is induced in the presence of nonsteroidal anti-inflammatory drugs or glucocorticoids (52,53), suggesting that it may play a role in the anti-inflammatory response. Candidate mediators might include conjugated steroids, which are substrates of ABCC3 (54). Dampened efflux of an antiproliferative or anti-inflammatory mediator might be expected to contribute to a proinflammatory environment otherwise promoted by high levels of ABCC1 and ABCC4.

The coordinate expression of high levels of *ABCC1* and *ABCC4* and low levels of *ABCC3* in poor outcome neuroblastoma is likely to reflect a common regulatory mechanism. We have recently found that MYCN positively regulates the expression of *ABCC1* and *ABCC4*, and negatively regulates *ABCC3*, but does not regulate other members of the ABCC subfamily (8). Direct regulation by MYCN raises the possibility that these transporters are important contributors to a transcriptional program that facilitates development of aggressive treatment-refractory neuroblastoma.

A limitation of this study is that although robust cellular phenotypes are observed upon suppression of ABCC4 or enhanced expression of ABCC3 in vitro, the implications for neuroblastoma tumor biology remain to be confirmed in vivo. In this respect, in vivo experiments analogous to those presented here for ABCC1 are currently being undertaken. Also, although each of these transporters clearly can contribute to various cellular phenotypes, the precise cellular mechanisms by which they do so are still the subject of ongoing studies.

In conclusion, our results indicate that ABCC1 contributes to the development of neuroblastoma in a mouse model and suggest that this occurs through contributions to fundamental processes within the tumor cell, independent of its established drug efflux role. Furthermore, our results suggest that ABCC4 and ABCC3 also contribute directly to neuroblastoma outcome, again independent of drug efflux. Given the powerful prognostic significance of these three ABCC genes, further investigation of their fundamental roles in tumor biology is clearly warranted, and with the current and evolving use of ABCC1 and ABCC4 substrate drugs in neuroblastoma, a case is building for development of targeted therapeutics against these transporters or against pathways associated with their biological functions. Elucidation of such pathways is the subject of ongoing studies aimed at identifying the precise endogenous substrates responsible for the observed effects on tumorigenesis and neuroblastoma cell biology. This study also highlights the advantages of broadening expression studies beyond those ABC transporters expected to mediate drug resistance in a particular tumor type.

References

1. Brodeur GM. Neuroblastoma: biological insights into a clinical enigma. *Nat Rev Cancer.* 2003;3(3):203–216.
2. Brodeur GM, Castleberry RP. Neuroblastoma. In: Pizzo PA, Poplack DG, eds. *Principles and Practices of Pediatric Oncology*. Philadelphia, PA: Lippincott-Raven; 1997:761–791.
3. Seeger RC, Brodeur GM, Sather H, et al. Association of multiple copies of the N-*myc* oncogene with rapid disease progression of neuroblastomas. *N Engl J Med.* 1985;313(18):1111–1116.
4. Munoz M, Henderson M, Haber M, Norris M. Role of the MRP1/ABCC1 multidrug transporter protein in cancer. *IUBMB Life.* 2007;59(12):752–757.
5. Haber M, Smith J, Bordow SB, et al. Association of high-level MRP1 expression with poor clinical outcome in a large prospective study of primary neuroblastoma. *J Clin Oncol.* 2006;24(10):1546–1553.
6. Norris MD, Bordow SB, Marshall GM, et al. Expression of the gene for multidrug-resistance-associated protein and outcome in patients with neuroblastoma. *N Engl J Med.* 1996;334(4):231–238.
7. Manohar CF, Bray JA, Salwen HR, et al. MYCN mediated regulation of the MRP1 promoter in human neuroblastoma. *Oncogene.* 2004;23(3):753–762.
8. Porro A, Haber M, Diolaiti D, et al. Direct and coordinate regulation of ATP-binding cassette transporter genes by Myc factors generates specific transcription signatures that significantly affect the chemoresistance phenotype of cancer cells. *J Biol Chem.* 2010;285(25):19532–19543.
9. Deeley RG, Westlake C, Cole SP. Transmembrane transport of endo- and xenobiotics by mammalian ATP-binding cassette multidrug resistance proteins. *Physiol Rev.* 2006;86(3):849–899.
10. Burkhart CA, Watt F, Murray J, et al. Small-molecule multidrug resistance-associated protein 1 inhibitor reversan increases the therapeutic index of chemotherapy in mouse models of neuroblastoma. *Cancer Res.* 2009;69(16):6573–6580.

11. Fletcher JI, Haber M, Henderson MJ, Norris MD. ABC transporters in cancer: more than just drug efflux pumps. *Nat Rev Cancer.* 2010;10(2): 147–156.
12. Norris MD, Smith J, Tanabe K, et al. Expression of multidrug transporter MRP4/ABCC4 is a marker of poor prognosis in neuroblastoma and confers resistance to irinotecan in vitro. *Mol Cancer Ther.* 2005;4(4):547–553.
13. Weiss W, Aldape K, Mohapatra G, Feuerstein B, Bishop J. Targeted expression of MYCN causes neuroblastoma in transgenic mice. *EMBO J.* 1997;16(11):2985–2995.
14. Burkhart CA, Cheng AJ, Madafiglio J, et al. Effects of MYCN antisense oligonucleotide administration on tumorigenesis in a murine model of neuroblastoma. *J Natl Cancer Inst.* 2003;95(18):1394–1403.
15. Lorico A, Rappa G, Finch RA, et al. Disruption of the murine MRP (multidrug resistance protein) gene leads to increased sensitivity to etoposide (VP-16) and increased levels of glutathione. *Cancer Res.* 1997;57(23): 5238–5242.
16. Ross RA, Spengler BA, Biedler JL. Coordinate morphological and biochemical interconversion of human neuroblastoma cells. *J Natl Cancer Inst.* 1983;71(4):741–747.
17. Spengler BA, Ross RA, Biedler JL. Differential drug sensitivity of human neuroblastoma cells. *Cancer Treat Rep.* 1986;70(8):959–965.
18. Reid G, Wielinga P, Zelcer N, et al. The human multidrug resistance protein MRP4 functions as a prostaglandin efflux transporter and is inhibited by nonsteroidal antiinflammatory drugs. *Proc Natl Acad Sci U S A.* 2003;100(16):9244–9249.
19. Payen L, Gao M, Westlake C, et al. Functional interactions between nucleotide binding domains and leukotriene C4 binding sites of multidrug resistance protein 1 (ABCC1). *Mol Pharmacol.* 2005;67(6):1944–1953.
20. Ilias A, Urban Z, Seidl TL, et al. Loss of ATP-dependent transport activity in pseudoxanthoma elasticum-associated mutants of human ABCC6 (MRP6). *J Biol Chem.* 2002;277(19):16860–16867.
21. Murphy KM, Streips UN, Lock RB. Bax membrane insertion during Fas(CD95)-induced apoptosis precedes cytochrome c release and is inhibited by Bcl-2. *Oncogene.* 1999;18(44):5991–5999.
22. Grant CE, Valdimarsson G, Hipfner DR, et al. Overexpression of multidrug resistance-associated protein (MRP) increases resistance to natural product drugs. *Cancer Res.* 1994;54(2):357–361.
23. Verrills NM, Po'uha ST, Liu ML, et al. Alterations in gamma-actin and tubulin-targeted drug resistance in childhood leukemia. *J Natl Cancer Inst.* 2006;98(19):1363–1374.
24. Schmittgen TD, Livak KJ. Analyzing real-time PCR data by the comparative C(T) method. *Nat Protoc.* 2008;3(6):1101–1108.
25. Kaplan EL, Meier P. Nonparametric estimation from incomplete observations. *J Am Stat Assoc.* 1958;53(282):457–481.
26. Peto R, Peto J. Asymptotically efficient rank invariant test procedures. *J R Stat Soc Ser A.* 1972;135(2):185–198.
27. Oberthuer A, Berthold F, Warnat P, et al. Customized oligonucleotide microarray gene expression-based classification of neuroblastoma patients outperforms current clinical risk stratification. *J Clin Oncol.* 2006;24(31): 5070–5078.
28. London WB, Castleberry RP, Matthay KK, et al. Evidence for an age cutoff greater than 365 days for neuroblastoma risk group stratification in the Children's Oncology Group. *J Clin Oncol.* 2005;23(27):6459–6465.
29. Peaston AE, Gardaneh M, Franco AV, et al. MRP1 gene expression level regulates the death and differentiation response of neuroblastoma cells. *Br J Cancer.* 2001;85(10):1564–1571.
30. Smith AG, Popov N, Imreh M, Axelson H, Henriksson M. Expression and DNA-binding activity of MYCN/Max and Mnt/Max during induced differentiation of human neuroblastoma cells. *J Cell Biochem.* 2004;92(6): 1282–1295.
31. Szakacs G, Paterson JK, Ludwig JA, Booth-Genthe C, Gottesman MM. Targeting multidrug resistance in cancer. *Nat Rev Drug Discov.* 2006; 5(3):219–234.
32. van de Ven R, Scheffer GL, Scheper RJ, de Gruijl TD. The ABC of dendritic cell development and function. *Trends Immunol.* 2009;30(9):421–429.
33. Berthold F, Hero B, Kremens B, et al. Long-term results and risk profiles of patients in five consecutive trials (1979-1997) with stage 4 neuroblastoma over 1 year of age. *Cancer Lett.* 2003;197(1–2):11–17.
34. Kuss BJ, Corbo M, Lau WM, et al. In vitro and in vivo downregulation of MRP1 by antisense oligonucleotides: a potential role in neuroblastoma therapy. *Int J Cancer.* 2002;98(1):128–133.
35. Borst P, de Wolf C, van de Wetering K. Multidrug resistance-associated proteins 3, 4, and 5. *Pflugers Arch.* 2007;453(5):661–673.
36. Tian Q, Zhang J, Chan SY, et al. Topotecan is a substrate for multidrug resistance associated protein 4. *Curr Drug Metab.* 2006;7(1):105–118.
37. Mantovani A, Allavena P, Sica A, Balkwill F. Cancer-related inflammation. *Nature.* 2008;454(7203):436–444.
38. Bergelin N, Blom T, Heikkila J, et al. Sphingosine kinase as an oncogene: autocrine sphingosine 1-phosphate modulates ML-1 thyroid carcinoma cell migration by a mechanism dependent on protein kinase C-alpha and ERK1/2. *Endocrinology.* 2009;150(5):2055–2063.
39. Nieuwenhuis B, Luth A, Chun J, et al. Involvement of the ABC-transporter ABCC1 and the sphingosine 1-phosphate receptor subtype S1P(3) in the cytoprotection of human fibroblasts by the glucocorticoid dexamethasone. *J Mol Med.* 2009;87(6):645–657.
40. Wijnholds J, Evers R, van Leusden MR, et al. Increased sensitivity to anticancer drugs and decreased inflammatory response in mice lacking the multidrug resistance-associated protein. *Nature Med.* 1997;3(11):1275–1279.
41. Gonzalez-Periz A, Claria J. New approaches to the modulation of the cyclooxygenase-2 and 5-lipoxygenase pathways. *Curr Top Med Chem.* 2007;7(3): 297–309.
42. Johnsen JI, Lindskog M, Ponthan F, et al. Cyclooxygenase-2 is expressed in neuroblastoma, and nonsteroidal anti-inflammatory drugs induce apoptosis and inhibit tumor growth in vivo. *Cancer Res.* 2004;64(20):7210–7215.
43. Robbiani DF, Finch RA, Jager D, et al. The leukotriene C(4) transporter MRP1 regulates CCL19 (MIP-3beta, ELC)-dependent mobilization of dendritic cells to lymph nodes. *Cell.* 2000;103(5):757–768.
44. Wielinga PR, van der Heijden I, Reid G, et al. Characterization of the MRP4- and MRP5-mediated transport of cyclic nucleotides from intact cells. *J Biol Chem.* 2003;278(20):17664–17671.
45. Sanchez S, Jimenez C, Carrera AC, et al. A cAMP-activated pathway, including PKA and PI3K, regulates neuronal differentiation. *Neurochem Int.* 2004;44(4):231–242.
46. Monaghan TK, Mackenzie CJ, Plevin R, Lutz EM. PACAP-38 induces neuronal differentiation of human SH-SY5Y neuroblastoma cells via cAMP-mediated activation of ERK and p38 MAP kinases. *J Neurochem.* 2008;104(1):74–88.
47. Kis B, Isse T, Snipes JA, et al. Effects of LPS stimulation on the expression of prostaglandin carriers in the cells of the blood-brain and blood-cerebrospinal fluid barriers. *J Appl Physiol.* 2006;100(4):1392–1399.
48. Rius M, Hummel-Eisenbeiss J, Keppler D. ATP-dependent transport of leukotrienes B4 and C4 by the multidrug resistance protein ABCC4 (MRP4). *J Pharmacol Exp Ther.* 2008;324(1):86–94.
49. Zelcer N, Reid G, Wielinga P, et al. Steroid and bile acid conjugates are substrates of human multidrug-resistance protein (MRP) 4 (ATP-binding cassette C4). *Biochem J.* 2003;371(pt 2):361–367.
50. Greenhough A, Smartt HJ, Moore AE, et al. The COX-2/PGE2 pathway: key roles in the hallmarks of cancer and adaptation to the tumour microenvironment. *Carcinogenesis.* 2009;30(3):377–386.
51. Wang MT, Honn KV, Nie D. Cyclooxygenases, prostanoids, and tumor progression. *Cancer Metastasis Rev.* 2007;26(3–4):525–534.
52. Pulaski L, Kania K, Ratajewski M, et al. Differential regulation of the human MRP2 and MRP3 gene expression by glucocorticoids. *J Steroid Biochem Mol Biol.* 2005;96(3–4):229–234.
53. Tatebe S, Sinicrope FA, Kuo MT. Induction of multidrug resistance proteins MRP1 and MRP3 and gamma-glutamylcysteine synthetase gene expression by nonsteroidal anti-inflammatory drugs in human colon cancer cells. *Biochem Biophys Res Commun.* 2002;290(5):1427–1433.
54. Borst P, Zelcer N, van de Wetering K. MRP2 and 3 in health and disease. *Cancer Lett.* 2006;234(1):51–61.

Funding

National Health and Medical Research Council, Australia (350885, 401129, 630608) Cancer Institute New South Wales, Australia (05/RIG/1-30); Cancer Council New South Wales, Australia (PG/05/00); National Cancer Institute, USA (CA29139); National Institutes of Health, USA; Children's Oncology Group,

USA; Italian Association for Research on Cancer, Italy; Italian Ministry of University and Research, Italy; and University of Bologna, Italy. The authors declare no competing financial interests.

Notes

M. J. Henderson, M. Haber and A. Porro contributed equally to this work. G. Perini and M. D. Norris contributed equally to this work. Children's Cancer Institute Australia for Medical Research is affiliated with the University of New South Wales and Sydney Children's Hospital, Randwick, Sydney, Australia. The funders did not have any involvement in the design of the study; the collection, analysis, and interpretation of the data; the writing of the article; or the decision to submit the article for publication.

Affiliations of authors: Experimental Therapeutics and Molecular Diagnostics Program, Children's Cancer Institute Australia for Medical Research, Lowy Cancer Research Centre, University of New South Wales, Randwick, NSW, Australia (MJH, MH, MAM, CX, JM, CLF, JS, JIF, C-KK, AJR, LJA, MDN); Molecular Carcinogenesis Program, Children's Cancer Institute Australia for Medical Research, Lowy Cancer Research Centre, University of New South Wales, Randwick, NSW, Australia (GMM); Formerly of Department of Biology, University of Bologna, Bologna, Italy (AP); ISREC-Swiss Institute for Experimental Cancer Research, Ecole Polytechnique Federale de Lausanne, Lausanne, Switzerland (AP); Department of Biology, University of Bologna, Bologna, Italy (NI, SG, EV, GP); Department of Biostatistics, Children's Oncology Group Statistics and Data Center, Dana-Farber Harvard Cancer Care and Children's Hospital Boston, Boston, MA (WBL); CureSearch, Children's Oncology Group Statistics and Data Center, Arcadia, CA (ABB); Department of Pharmacology, Yale University School of Medicine, New Haven, CT (ACS); Department of Pediatrics, The University of Chicago, Chicago, IL (SLC); Division of Tumor Genetics, German Cancer Research Center (DKFZ), Heidelberg, Germany (MS).